ACS APPLIED NANO MATERIALS
Cite This: ACS Appl. Nano Mater. 2019, 2, 1713−1719
Article
www.acsanm.org

Enhancement of Electrochromic Polymer Switching in Plasmonic Nanostructured Environment

Mohammad Shahabuddin,* Thomas McDowell, Carl E. Bonner, and Natalia Noginova

Center for Materials Research, Norfolk State University, 700 Park Ave., Norfolk, Virginia 23504, United States

ABSTRACT: We explore color switching properties of thin polyaniline (PANI) films deposited on plasmonic nanomesh structures in comparison with the films deposited on flat gold. The nanostructured systems show a much steeper color switching with increasing voltage than the films prepared on flat substrates. A strong difference between nanostructured and flat systems is also observed at small voltages, where nanostructured samples often demonstrate an additional feature in cyclic voltammetry curves and nonmonotonous changes in optical properties. Possible origins of the observed effects are discussed in terms of acceleration of charge transport in nanostructured plasmonic environment and interface-related effects. The results can provide opportunities for enhancing and controlling the electrochromic polymer performance in smart windows or display applications.

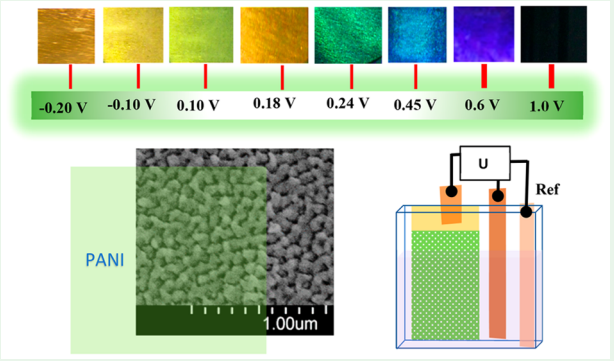

KEYWORDS: *plasmonics, charge transfer, nanostructures, cyclic voltammetry*

INTRODUCTION

Electrochromic materials show a reversible color change upon reduction or oxidation of the material by the application of a small voltage and present interest for optoelectronics and flexible display applications.[1,2] During the reduction or oxidation processes, the dielectric functions of the electrochromic material can be altered to a large extent and their absorption colors can be varied. Electrochromic switching is a complex process, involving changes in the oxidation states, redox reactions with gain or loss of electrons, and the simultaneous insertion/extraction of ions with opposite charges to balance internally created electric fields.[3] The electrochromic performance often relies on the kinetics of charge transport, including the electron diffusion in electrochromic materials as well as ion transport in the electrolyte, in electrochromic materials, and at their interfaces.[4]

Electrochromic color switching has been observed in many materials, such as Prussian Blue and other metal metallohexacyanates, viologens, metal hydrides, transition-metal complexes, and conjugated polymers, including polyaniline (PANI).[5−7] Polyaniline has three well-defined oxidation states, which are leucoemeraldine (the fully reduced, poorly conducting state), emeraldine (the half oxidized, highly conducting state), and pernigraniline (the fully oxidized, poorly conducting state), with a substantially infinite number of possible oxidation states prevailing in between. With an increase of the electrode potential, the color of the polyaniline film changes from transparent yellow to green, green to blue, and blue to blue-violet and turns to black at higher potential, and vice versa.[3]

A typical cyclic voltammetry (CV) curve of polyaniline has two major pairs of anodic and cathodic current peaks (Figure 1). The first pair of peaks (O_1, R_1) is associated with the conversion from the fully reduced leucoemeraldine base to the partially oxidized emeraldine and back, and the second set of redox current peaks (O_2, R_2) corresponds to the conversion between emeraldine and fully oxidized pernigraniline. An additional intermediate peak between the previous two peaks is attributed to the formation of electrochemically inactive quinonediimine structures.[8−12]

PANI is promising for electrochromic applications because of easy facile polymerization in aqueous or nonaqueous media, high coloration efficiencies, fast response speeds, flexibility, good stability in air, low cost, and high conductivity.[13−16] In addition, polyaniline forms a scatter-free uniform thin layer on metallic structures through electrochemical deposition, whereas deposition of transition metal oxide, Prussian Blue, and other inorganic electrochromic materials often results in nanocrystal formation which causes undesired scattering.[17,18] However, it still suffers from several disadvantages, which restricts the breadth of applications. A single type of polymer cannot cover the full visible range, and a thick layer is required to maintain high contrast, which leads to a long switching time, $\tau \propto L^2/D$, where L is the film thickness and D is the ionic diffusivity. Finally, the relatively high electrochemical potential required for high color contrast can deteriorate the polymers.

Received: January 24, 2019
Accepted: February 14, 2019
Published: February 14, 2019

DOI: 10.1021/acsanm.9b00147
ACS Appl. Nano Mater. 2019, 2, 1713−1719

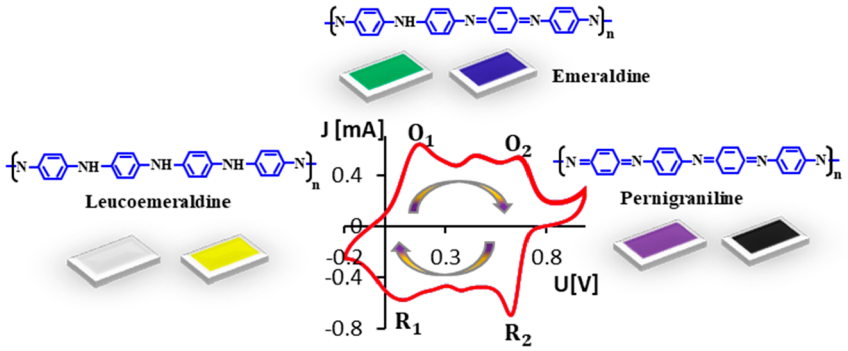

Figure 1. Polyaniline states and color switching during cyclic voltammetry experiment.

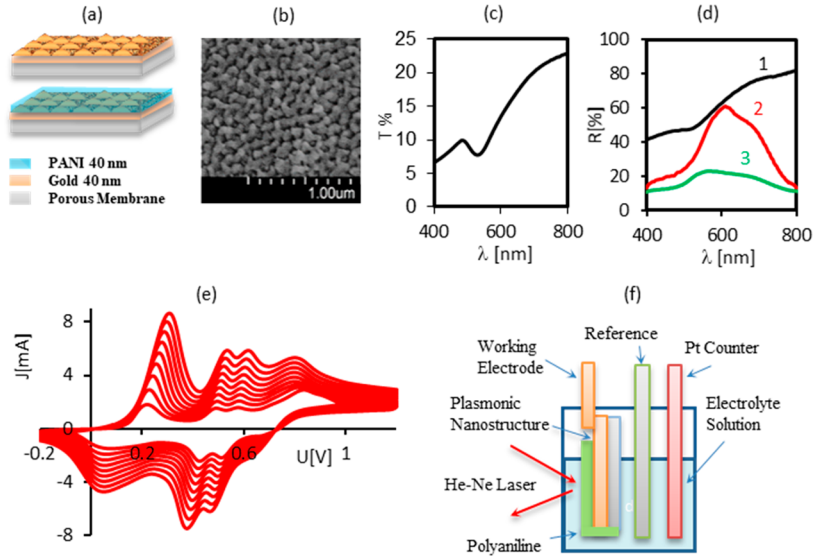

Figure 2. (a) Schematic of the gold nanomesh substrate without (top) and with PANI (bottom). (b) SEM image of nanomesh gold with periodicity of 100 nm. (c) Optical transmission spectrum of the substrate. (d) Reflection spectra of the substrate in electrolyte without (trace 1) and with PANI at zero voltage (trace 2) and 0.5 V (trace 3). (e) CV curves during PANI deposition. (f) Schematics of the CV experiment with simultaneous recording of changes in optical reflectivity.

Different approaches are taken to improve the switching performance of PANI, such as use of multilayer structures, which can bring faster color switching with the mitigation of color contrast.[19] Recent research[20−24] points to a very interesting possibility of enhancing PANI switching with plasmonic nanostructures. Specifically, incorporation of PANI into metallic nanoslit arrays enables control of color with slit dimensions and demonstrates faster electrochromic switching.[20] In addition, plasmonic structures support tight spatial confinement and high local field intensity associated with the plasmonic fields, allowing for the usage of extremely thin layers of the active materials to achieve high optical contrast. Other studies have shown that the plasmonic resonance can be tuned electrically by embedding plasmonically active noble metal nanostructure (including gold nanocube[21,23] and nanorod[22,24]) into the electrochromic polymer. The application of electric potential in the electroactive media alters the refractive indices of responsive materials, which can lead to the electrical control of plasmonic resonances.

Plasmonic metamaterials and metasurfaces can bring additional opportunities associated with strong modification of local dielectric environment in close vicinity of such systems. The effects are commonly discussed in terms of the modification in the density of photonic states determining various quantum processes. Acceleration in the spontaneous emission rate (Purcell effect),[25−29] changes in the Förster energy transfer rate,[30,31] and modification of the photochemical reactions[32] were reported in the vicinity of plasmonic systems and metamaterials. Photoinduced electric effects in nanoscale metal systems also include generation of dc electric voltages or currents[33,34] and generation of hot electrons.[35−41] Under conditions of plasmon resonance, a metal particle acts as a source of electrons, which are strongly accelerated by plasmonic fields and escape along the trajectories governed by the particle geometry.[35] Novel effects associated with catalytic activity of hot electrons are reported.[36−41]

The effects of plasmonic environment on charge transport and color switching of PANI are not yet fully studied and understood. To get more information about this subject, we further explore oxidation/reduction reactions in PANI in plasmonic environment and compare the effects observed in thin PANI films deposited on gold nanomesh structures (Figure 2a) with those deposited on flat gold.

EXPERIMENTAL SECTION

Flat and nanostructured Au films are prepared by thermal deposition of gold (40 nm thick) onto precleaned glass substrates and nanoporous anodic aluminum oxide (AAO) substrates precoated

DOI: 10.1021/acsanm.9b00147
ACS Appl. Nano Mater. 2019, 2, 1713−1719

with a 3 nm thick Cr adhesion layer. The deposition of gold onto AAO substrate produces highly nanostructured surfaces (Figure 2b). Such nanomesh is expected to show multiple plasmon resonances which can be excited with direct illumination. Similar systems were used in ref 33, where they demonstrated plasmon-related electric effects under pulse laser light illumination in the broad optical range (400−700 nm). The presence of localized plasmon resonances can be clearly seen as a well-defined dip in the transmission spectrum at λ = ∼537 nm (Figure 2c). The reflection spectrum (Figure 2d) of the nanomesh shows plasmon related features as well, including a dip at ∼530 nm, which is due to localized plasmons, and a broader feature at 700 nm, which depends on the periodicity of the membrane and can be tentatively ascribed to collective modes. However, after PANI deposition, the reflection spectrum is mostly determined by optical properties of PANI (Figure 2d, traces 2 and 3).

PANI films are deposited with the electrochemical method[42,43] by sweeping the potential between −0.2 and 1.2 V at a scan rate of 30 mV s^{-1} in an aqueous solution containing 0.1 M aniline and 2 M HNO_3. In our fabrication, we deposit polyaniline on both flat gold and nanomesh gold surface at the same time and setup. A Pt rod is used as a counter electrode, and Ag/AgCl is used as a reference electrode. The film growth is verified by the increased current with increasing the number of CV cycles (see Figure 2e). Obtained films are washed with monomer-free electrolyte solution. The thickness of the film on flat gold is measured using a profilometer. Because polyaniline is deposited onto both flat gold and gold nanomesh substrates exactly at the same environment, the thicknesses of both layers are expected to be approximately same. Most experiments are performed with films of ∼40 nm thickness. The schematics of the PANI/nanomesh system is illustrated in Figure 2a.

In the cyclic voltammetry and reflectivity experiments (see the setup in Figure 2f), we study changes in coloration as a response to applied potential in the circular voltammetry setup, simultaneously recording both electric current and the optical reflectivity, R, as a function of the voltage. The flat and nanomesh gold substrates are used as a working electrode along with a Pt counter electrode and a reference Ag/AgCl electrode. All measurements are taken with the electrolyte solution of the same content (of 0.1 mol/L HNO_3 and 1 mol/L $NaNO_3$) and in the same cell geometry. The CV curves are recorded with a Biologic SP-300 potentiostat. For the reflectivity measurements, the sample is illuminated at 632.8 nm using the light of a HeNe laser. This wavelength corresponds to strong variations in coloration with applied voltage.[3] The reflected light is collected with an integration sphere and recorded with the Tektronix oscilloscope as a function of time together with the output signal (voltage) from the CV instrument. Then the experimental data on both electric current and reflectivity are plotted and analyzed as a function of the applied potential.

In the experiments, we use various scan speeds and potential sweeping ranges. Main results are obtained at the rate of the voltage scan of 30 mV/s. Further slowdown of the rate (10 mV/s) practically does not affect the results while at a faster rate (100 mV/s), the $I-V$ and $R-V$ curves show significant modification. The positions of the peaks are also pH independent of electrolyte solution.

RESULTS

Typical results are shown in Figures 3 and 4 for the voltage sweeps of −0.4 to +0.4 V and −0.2 to +1 V, respectively. In the first case (Figure 3), the PANI films are not expected to fully oxidize to the pernigraniline states and thus avoid polymer degradation over many switching cycles. The larger sweep (−0.2 to +1 V) reveals the third intermediate peak (associated with formation of quinonediimine) and shows a hysteresis in $R-V$ dependence (Figure 4).

As one can see, in both cases the voltage−current dependences and color switching behavior are significantly different in the nanomesh and flat gold structures. The films on nanostructured gold demonstrate much steeper changes in

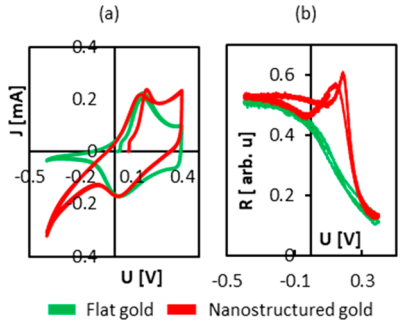

Figure 3. (a) Cyclic voltammetry ($I-V$ dependence) and (b) reflectance vs voltage in flat and nanostructured gold with PANI at the voltage sweep from −0.4 to 0.4 V.

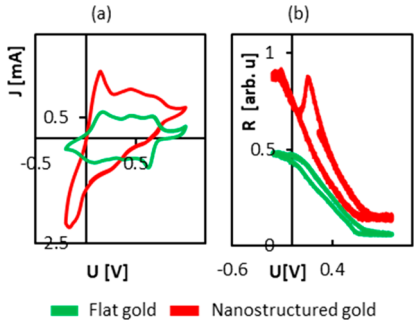

Figure 4. (a) Cyclic voltammetry ($I-V$ dependence) and (b) reflectance vs voltage in flat and nanostructured gold with PANI at the voltage sweep from −0.2 to 1 V.

reflection with the increase in voltage than those on the flat gold. A special feature of the nanomesh systems is a small reflectivity peak observed around 0.2 V, which is not present in the flat gold. At small voltages, the reflectivity of the PANI/nanomesh system first increases with the increase in voltage and then sharply decreases, while the decrease in reflectivity is much gradual in PANI on flat gold.

At the same time, the positions of oxidation peaks in nanomesh and flat gold systems are similar to each other. In Figure 3a, the peak O_1 at 0.2 V is observed in CV curves of both flat and nanomesh systems, which nominally corresponds to the change of polyaniline state from lucomeraldine to emeraldine.[46,47] At a larger voltage scan range (Figure 4), the difference between the systems becomes more prominent. In $I-V$ curves, in PANI on flat gold the first oxidation peak, O_1, is observed at 0.2 V, whereas in the nanomesh structure the first peak is observed between 0.1 and 0.15 V, which is much lower than the reported values[8,48−50] for the polyaniline. Note that a slight shift of the oxidation peak has been reported in polyaniline hybrids[51] and polyaniline nanocomposites;[13] however, the peak was still around 0.2 V. The pair of peaks O_2, R_2 (emeraldine−pernigraniline conversion) is observed at ∼0.7 V for the both types of structures. Similar values for the both systems (∼0.4 V) are seen for the position of the intermediate oxidation peak as well in accordance with the reported values.[52−54] However, the reduction peak, R_1, is significantly shifted to the negative voltages (relative to Ag/AgCl) in the nanomesh system. Note that the positions of the low-voltage peaks in the CV curve of PANI/nanomesh correlate with the positions of the reflectivity peaks in the $R-V$ curve.

DOI: 10.1021/acsanm.9b00147
ACS Appl. Nano Mater. 2019, 2, 1713−1719

To better understand the reverse behavior in $R-V$ curves observed at small voltages in nanostructured systems, a hand-held camera is used to capture the image of the electrochromic cell with PANI/flat gold (Figure 5) and PANI/nanomesh (Figure 6) electrodes during the CV experiment.

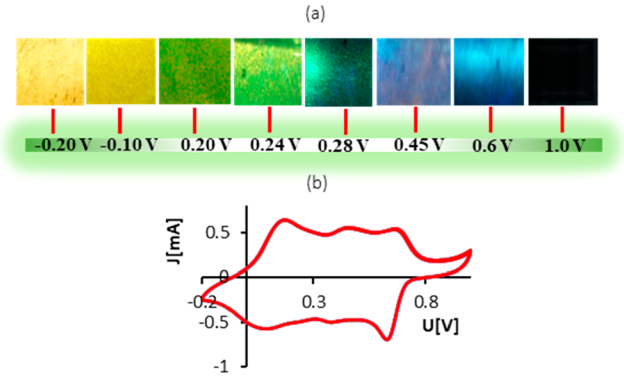

Figure 5. Electrochromic experiment in PANI on flat gold. (a) Change of coloration with applied potential; (b) corresponding CV curve.

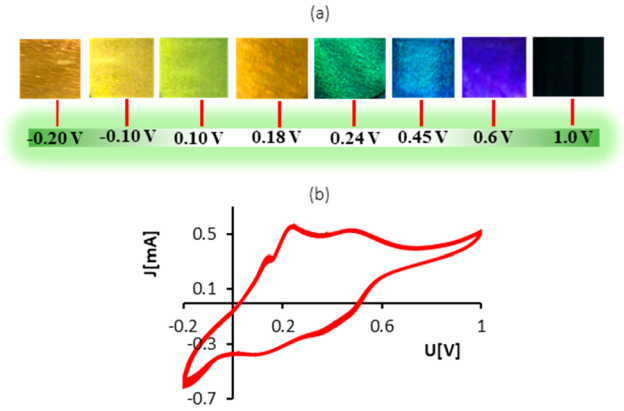

Figure 6. Electrochromic experiment of PANI on gold nanomesh. (a) Change of coloration with applied potential; (b) corresponding CV curve.

As one can see in Figure 5, PANI/flat gold system demonstrates the coloration switching which is well expected and corresponds to that described in the literature. The PANI film is transparent and yellow at small voltages and gradually changes to green at 0.2 V, blue at around 0.5 V, and dark at high voltages.

Figure 6 shows the high contrast, distinguishable, and fully reversible vibrant color of the PANI-nanomesh cell at different voltages. In comparison with PANI/flat gold, the coloration behavior in the PANI/nanomesh system is significantly different. With increasing the applied voltage from −0.2 to +0.2 V, the color of the system changes respectively from brownish to yellow, light yellow, and then to brownish again. A slight increment of applied potential over 0.18 V turns the cell color into deep green at 0.22 V. With the further increase in the potential, the coloration quickly switches over a broad range of colors from green to blue, violet, and dark.

Note that the onset of strong color changes in the PANI/nanomesh system corresponds to a small additional peak in the CV curve (Figure 6b), which is clearly seen in this particular sample. This peak is separate from the first oxidation peak. No such peak is observed in PANI/flat gold systems.

Note that, the thicknesses of polyaniline deposited on flat gold and nanomesh gold are the same and the reflection studies are performed with the identical experimental setup for the electrochromic switching. The observed differences between reflectance maxima and minima are about 70% for gold nanomesh cell and 40% for flat gold cell (Figure 4b). This indicates the possibility of gaining a high figure-of-merit and high contrast of polyaniline for display applications through the plasmonic metasurface.

This reverse coloration behavior observed at small voltages in PANI/nanomesh is an intriguing finding. Instead of a gradual increase in coloration with the increasing voltage (as observed in PANI on flat gold), PANI/nanomesh first becomes more transparent until a certain voltage, and only after that it demonstrates sharp color switching. To exclude a possible scenario that involves a simple interplay of the optical properties of the plasmonic substrate and PANI, the reflectance spectra of flat and nanostructured systems are recorded in a UV−vis PerkinElmer spectrophotometer using a electrochromic cell with the electrolyte solution and varying voltage between two electrodes. (No reference electrode is used in this experiment.) In similarity with refs 44 and 45, application of the positive potential to the electrode with PANI leads to gradual and monotonous coloration changes and a corresponding decrease in the reflection in the flat gold structures (see Figure 7a). In PANI with gold nanomesh, the situation is different, demonstrating nonmonotonous behavior

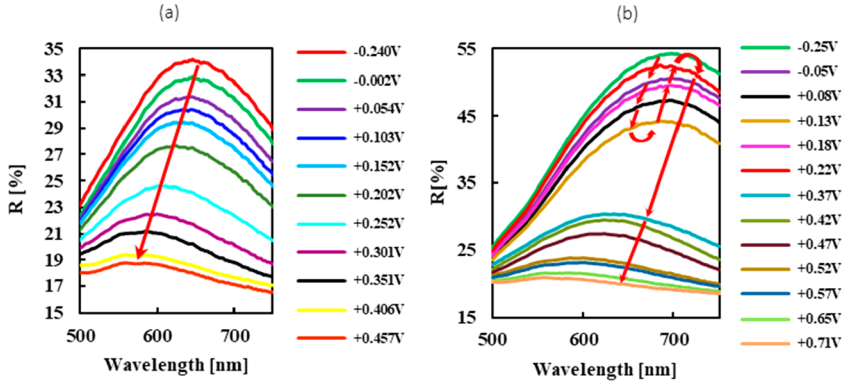

Figure 7. (a) UV−vis reflection spectra of PANI deposited on flat gold at different voltages. (b) UV−vis reflection spectra of PANI deposited on gold nanomash at different voltages. The red arrows show direction of changes in the reflection spectra with increasing electrode potential.

DOI: 10.1021/acsanm.9b00147
ACS Appl. Nano Mater. 2019, 2, 1713−1719

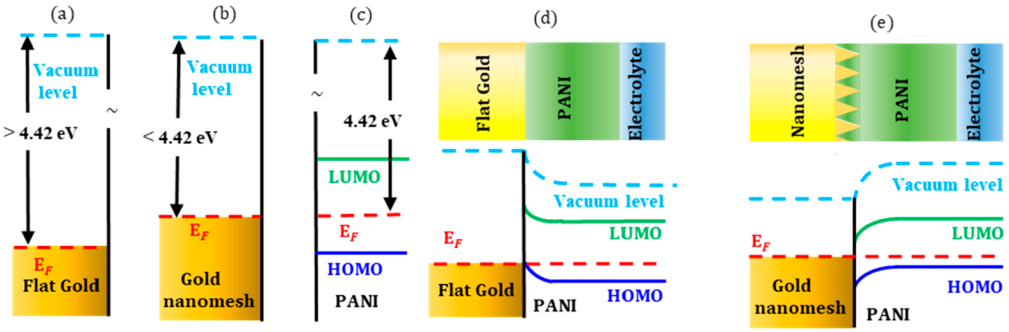

Figure 8. Energy band diagrams of (a) flat gold, (b) gold nanomesh, and (c) PANI. (d) Formation of ohmic contact at flat gold/PANI interface. (e) Formation of Schotky barrier at gold nanomesh/PANI interface.

and drastic changes in the coloration with the increase in the voltage (see Figure 7b). First, with the increase of the electrode potential up to ~0.13 V, the intensity of the reflection spectra decreases as expected. However, the further increment of the potential increases the reflection toward the local maximum at about +0.22 V; afterward, a slight increment of electrode potential leads to a sharp drop in the reflection toward the asymptotic minimum in the reflection intensity. Note that those changes are observed in the broad spectral range without any noticeable resonance-related features. The spectral maximum of the reflection demonstrates a blue-shift with the increase in the potential, being monotonous in the flat system and nonmonotonous in the nanomesh structure.

DISCUSSION

Steeper color switching and saturation at moderate voltages observed in the nanostructured gold correlate with the results of ref 20, where acceleration and strong contrast of PANI switching were observed in plasmonic cavities. Our results indicate that the modification of electrochemical switching is a general effect associated with plasmonic nanostructured environment. One of the possible factors discussed in the literature is the modification of the charge transport kinetics.[55,56] The plasmonic nanostructures often offers remarkably high surface areas, increasing the electrode−electrolyte surface area and maximizing specific capacity of the electrode, leading to mostly capacitively injected charge flow.

Our experiments in PANI/nanomesh systems demonstrate strongly asymmetric *I*−*V* curves and unusual coloration behavior at low voltages. We believe that such a behavior can primarily be related to the interface effects.[56] Figure 8 illustrates energy band diagrams of gold, gold nanomesh, and PANI and effects on the interfaces of PANI/gold and PANI/nanomesh systems. According to refs 57−59, PANI is a p-type semiconductor with the work function of 4.42−4.78 eV,[60] which would form the Schottky contact with metal if its work function is lower than that and the Ohmic contact in the opposite case. While in gold the work function is of 5.3 eV,[61] in nanostructured gold it can be significantly lower. Values of 3.6 and 3.4 eV were reported in gold nanoparticles.[62,63] In this case, the barrier and a depletion layer in PANI are expected to form, affecting it is electrical and optical properties. A nice agreement is found in ref 64, which indicates that PANI shows the Schottky junction properties for metal/PANI/metal combination with Pb, Sn, In, Sb, and Al (work functions are 4.02, 4.11, 4.12, 4.05, and 3.74 eV, respectively) where Ag is used as Ohmic contact. The rectifying behavior has been reported[59,64] at the organic−inorganic interface formed at PANI/metal junction. For the Schottky interface, application of voltage in the forward direction reduces the barrier height; at a threshold voltage the charge carriers can breach the barrier height, leading to strong increase of the current. This consideration can be applied to explain the additional current peak (or enhanced O_1 peak) at small voltages observed in the forward part of the cyclic voltammogram for the gold nanomesh/PANI cell in Figures 4a and 6b. During the reverse part of the cyclic voltammogram, the potential barrier is higher, and no such interface-related current peak is observed in the cyclic voltammogram.

The possibility to control the interface effects with nanostructuring in combination with acceleration of switching properties can open new applications for electrochromic polymers in electronics and optoelectronics. A plasmonic environment provides another interesting opportunity, related to "plasmogalvanic" effects.[65] According to ref 66, an excitation of plasmon resonances leads to charging of plasmonic nanofeatures,[66] which can be controlled with light illumination wavelength and intensity. The experiments are underway.

In conclusion, electrochromic polyaniline deposited on a gold nanomesh demonstrates high contrast colors, which can be electrochemically switched with applied potential. The switching behavior in nanostructured systems is significantly different than in PANI/flat gold structures, featuring the onset of steep changes in the coloration with increasing voltage above 0.15−0.2 V, the presence of an additional peak in the voltage−current curves, and reverse coloration behavior at small voltages. The effects are tentatively attributed to the role of the interface.

Our results are obtained in the reflection mode; however, we believe that enhancement of PANI performance with plasmonic nanostructures can be observed in transmission as well with slight modification in the setup. Instead of strongly scattering anodic alumina membranes, one can use a transparent substrate (glass, ITO, etc.) with a gold fishnet deposited onto it. The fabrication of such structure can be readily done using nanosphere template synthesis,[67] which allows covering of a large area with nanoscale features. Depending on the nanoscale geometry, such a structure is transparent in a certain range, which can be designed to match the range of electrochromic polymer operation. Possible applications include tunable optical filters, displays, and smart windows which can be electronically switched from the transparent state to various colors or turned dark for energy-saving applications. Other promising applications are in flexible electronic paper or wearable electrochromic displays.

DOI: 10.1021/acsanm.9b00147
ACS Appl. Nano Mater. 2019, 2, 1713−1719

As was shown recently,[68,69] the use of plasmonic nanostructured substrates in such applications can significantly improve the contrast and switching speed of the conjugate polymer.

AUTHOR INFORMATION

Corresponding Author

*E-mail m.shahabuddin@spartans.nsu.edu (M.S.).

ORCID

Mohammad Shahabuddin: 0000-0003-4357-3872

Funding

The work is supported by the Department of Defense (DoD Grant W911NF1810472), Airforce Office of Scientific Research (AFOSR Grant FA9550-18-0417), and National Science Foundation (Grants 1830886 and 1646789).

Notes

The authors declare no competing financial interest.

REFERENCES

(1) Eh, A. L. S.; Tan, A. W. M.; Cheng, X.; Magdassi, S.; Lee, P. S. Recent Advances in Flexible Electrochromic Devices: Prerequisites, Challenges, and Prospects. *Energy Technol.* **2018**, *6*, 33−45.

(2) Cai, G.; Wang, J.; Lee, P. S. Next-Generation Multifunctional Electrochromic Devices. *Acc. Chem. Res.* **2016**, *49*, 1469−1476.

(3) Mortimer, R. J.; Rosseinsky, D. R.; Monk, P. M. S. *Electrochromic Materials and Devices*; Willey Publications: 2015; Chapter 9, p 251.

(4) Liang, L.; Zhang, J.; Zhou, Y.; Xie, J.; Zhang, X.; Guan, M.; Pan, B.; Xie, Y. High Performance Flexible Electrochromic Device Based on Facile Semiconductor-to-Metal Transition Realized by WO_32H_2O Ultrathin Nanosheets. *Sci. Rep.* **2013**, *3*, 1936.

(5) Mortimer, R. Electrochromic Materials. *Chem. Soc. Rev.* **1997**, *26*, 147−156.

(6) Rowley, N. M.; Mortimer, R. J. New Electrochromic Materials. *Sci. Prog.* **2002**, *85* (3), 243−262.

(7) Somani, P. R.; Radhakrishnan, S. Electrochromic Materials and Devices: Present and Future. *Mater. Chem. Phys.* **2003**, *77*, 117−133.

(8) Song, E.; Choi, J. W. Conducting Polyaniline Nanowire and its Applications in Chemiresistive Sensing. *Nanomaterials* **2013**, *3* (3), 498−523.

(9) Watanabe, A.; Mori, K.; Iwasaki, Y.; Nakamura, Y.; Niizuma, S. Electrochromism of Polyaniline Film Prepared by Electrochemical Polarization. *Macromolecules* **1987**, *20*, 1793−1796.

(10) Focke, W. W.; Wnek, G. E.; Wei, Y. Influence of Oxidation State, pH, and Counterion on The Conductivity of Polyaniline. *J. Phys. Chem.* **1987**, *91*, 5813−5818.

(11) Saheb, A. H.; Seo, S. S. UV-vis and Raman Spectral Analysis of Polyaniline/Gold Thin Films as a Function of Applied Potential. *Anal. Lett.* **2011**, *44*, 1206−1216.

(12) Kobayashi, T.; Yoneyama, H.; Tamura, H. Electrochemical Reactions Concerned with Electrochromism of Polyaniline Film-Coated Electrodes. *J. Electroanal. Chem. Interfacial Electrochem.* **1984**, *177*, 281−291.

(13) Zhang, S.; Sun, G.; He, Y.; Fu, R.; Gu, Y.; Chen, S. Preparation, Characterization, and Electrochromic Properties of Nanocellulose Based Polyaniline Nanocomposite Films. *ACS Appl. Mater. Interfaces* **2017**, *9*, 16426−16434.

(14) Zhang, W.; Ju, W.; Wu, X.; Wang, Y.; Wang, Q.; Zhou, H.; Wang, S.; Hu, C. Structure, Stability and Electrochromic Properties of Polyaniline Film Covalently Bonded to Indium Tin Oxide Substrate. *Appl. Surf. Sci.* **2016**, *367*, 542−551.

(15) Meng, H.; Tucker, D.; Chaffins, S.; Chen, Y.; Helgeson, R.; Dunn, B.; Wudl, F. An Unusual Electrochromic Device Based on A New Low-Bangdgap Conjugated Polymer. *Adv. Mater.* **2003**, *15*, 146−149.

(16) Remmele, J.; Shen, D. E.; Mustonen, T.; Fruehauf, N. High Performance and Long-Term Stability in Ambiently Fabricated Segmented Solid-State Polymer Electrochromic Displays. *ACS Appl. Mater. Interfaces* **2015**, *7*, 12001−12008.

(17) Agrawal, A.; Susut, C.; Stafford, G.; Bertocci, U.; McMorran, B.; Lezec, H. J.; Talin, A. A. An Integrated Electrochromic Nanoplasmonic Optical Switch. *Nano Lett.* **2011**, *11*, 2774−2778.

(18) Guiseppi-Elie, A.; Pradhan, S. R.; Wilson, A. M.; et al. Growth of Electropolymerized Polyaniline Thin Films. *Chem. Mater.* **1993**, *5*, 1474−1480.

(19) Jain, V.; Yochum, H. M.; Montazami, R.; Heflin, J. R. Millisecond Switching in Solid State Electrochromic Polymer Devices Fabricated from Ionic Self-Assembled Multilayers. *Appl. Phys. Lett.* **2008**, *92*, 033304.

(20) Xu, T.; Walter, E. C.; Agrawal, A.; Bohn, C.; Velmurugan, J.; Zhu, W.; Lezec, H. J.; Talin, A. A. High-Contrast and Fast Electrochromic Switching Enabled by Plasmonics. *Nat. Commun.* **2016**, *7*, 10479.

(21) Jeon, J. W.; Ledin, P. A.; Geldmeier, J. A.; Ponder, J. F.; Mahmoud, M. A.; El-Sayed, M.; Reynolds, J. R.; Tsukruk, V. V. Electrically Controlled Plasmonic Behavior of Gold Nanocube@ Polyaniline Nanostructures: Transparent Plasmonic Aggregates. *Chem. Mater.* **2016**, *28*, 2868−2881.

(22) Jeon, J. W.; Zhou, J.; Geldmeier, J. A.; Ponder, J. F.; Mahmoud, M. A.; El-Sayed, M.; Reynolds, J. R.; Tsukruk, V. V. Dual-Responsive Reversible Plasmonic Behavior of Core−Shell Nanostructures with pH-Sensitive and Electroactive Polymer Shells. *Chem. Mater.* **2016**, *28*, 7551−7563.

(23) Konig, T. A. F.; Ledin, P. A.; Kerszulis, J.; Mahmoud, M. A.; El-Sayed, M. A.; Reynolds, J. R.; Tsukruk, V. V. Electrically Tunable Plasmonic Behavior of Nanocube-Polymer Nanomaterials Induced by a Redox-Active Electrochromic Polymer. *ACS Nano* **2014**, *8*, 6182−6192.

(24) Ledin, P. A.; Jeon, J. W.; Geldmeier, J. A.; Ponder, J. F.; Mahmoud, M. A.; El-Sayed, M.; Reynolds, J. R.; Tsukruk, V. V. Design of Hybrid Electrochromic Materials with Large Electrical Modulation of Plasmonic Resonances. *ACS Appl. Mater. Interfaces* **2016**, *8*, 13064−13075.

(25) Noginov, M. A.; Zhu, G.; Bahoura, M.; Small, C. E.; Davison, C.; Adegoke, J.; et al. Enhancement of Spontaneous and Stimulated Emission of a Rhodamine 6G Dye by an Ag Aggregate. *Phys. Rev. B: Condens. Matter Mater. Phys.* **2006**, *74*, 184203.

(26) Belacel, C.; Habert, B.; Bigourdan, F.; Marquier, F.; Hugonin, J. P.; Vasconcellos, S. M. D.; et al. Controlling Spontaneous Emission with Plasmonic Optical Patch Antennas. *Nano Lett.* **2013**, *13*, 1516−1521.

(27) Li, L.; Wang, W.; Luk, S. L.; Yang, X.; Gao, J. Enhanced Quantum Dot Spontaneous Emission with Multilayer Metamaterial Nanostructures. *ACS Photonics* **2017**, *4*, 501−508.

(28) Shubina, T. V.; Toropov, A. A.; Jmerik, V. N.; Kuritsyn, D. I.; Gavrilenko, L. V.; Krasil'nik, Z. F.; Araki, T.; Nanishi, Y.; Gil, B.; Govorov, A. O.; Ivanov, S. V. Plasmon-Induced Purcell Effect in InN/In Metal-Semiconductor Nanocomposites. *Phys. Rev. B: Condens. Matter Mater. Phys.* **2010**, *82*, 073304.

(29) Noginov, M. A.; Zhu, G.; Bahoura; Adegoke, M. J.; Small, C. E.; et al. Enhancement of Surface Plasmons in an Ag Aggregate by Optical Gain in a Dielectric Medium. *Opt. Lett.* **2006**, *31*, 20.

(30) Tumkur, T. U.; Kitur, J. K.; Bonner, C. E.; Poddubny, A. N.; Narimanov, E. E.; Noginov, M. A. Control of Forster Energy Transfer in the Vicinity of Metallic Surfaces and Hyperbolic Metamaterials. *Faraday Discuss.* **2015**, *178*, 395.

(31) Wubs, M.; Vos, W. L. Forster Resonance Energy Transfer Rate in any Dielectric Nanophotonic Medium with Weak Dispersion. *New J. Phys.* **2016**, *18*, 053037.

(32) Ueno, K.; Misawa, H. Surface Plasmon-Enhanced Photochemical Reactions. *J. Photochem. Photobiol., C* **2013**, *15*, 31−52.

(33) Noginova, N.; Rono, V.; Bezares, F. J.; Caldwell, J. D. Plasmon drag effect in metal nanostructures. *New J. Phys.* **2013**, *15*, 113061.

(34) Akbari, M.; Onoda, M.; Ishihara, T. Photo-induced voltage in nano-porous gold thin film. *Opt. Express* **2015**, *23*, 823.

DOI: 10.1021/acsanm.9b00147
ACS Appl. Nano Mater. 2019, 2, 1713−1719

(35) Linic, S.; Christopher, P.; Ingram, D. B. Plasmonic-Metal Nanostructures for Efficient Conversion of Solar to Chemical Energy. *Nat. Mater.* **2011**, *10*, 911−921.
(36) Govorov, A. O.; Zhang, H.; Demir, H. V.; Gun'ko, Y. K. Photogeneration of Hot Plasmonic Electrons with Metal Nanocrystals: Quantum Description and Potential Applications. *Nano Today* **2014**, *9*, 85−101.
(37) Brongersma, M. L.; Halas, N. J.; Nordlander, P. Plasmon-Induced Hot Carrier Science and Technology. *Nat. Nanotechnol.* **2015**, *10*, 25−34.
(38) Clavero, C. Plasmon-Induced Hot-Electron Generation at Nanoparticle/Metal-Oxide Interfaces for Photovoltaic and Photocatalytic Devices. *Nat. Photonics* **2014**, *8*, 95−103.
(39) Dombi, P.; Hörl, A.; Rácz, P.; Márton, I.; Trügler, A.; Krenn, J. R.; Hohenester, U. Ultrafast Strong-Field Photoemission from Plasmonic Nanoparticles. *Nano Lett.* **2013**, *13*, 674−678.
(40) Mukherjee, S.; Libisch, F.; Large, N.; Neumann, O.; Brown, L. V.; Cheng, J.; Lassiter, J. B.; Carter, E. A.; Nordlander, P.; Halas, N. J. Hot Electrons Do the Impossible: Plasmon-Induced Dissociation of H_2 on Au. *Nano Lett.* **2013**, *13*, 240−247.
(41) Lee, S. J.; Piorek, B. D.; Meinhart, C. D.; Moskovits, M. Photoreduction at a Distance: Facile, Nonlocal Photoreduction of Ag Ions in Solution by Plasmon-Mediated Photoemitted Electrons. *Nano Lett.* **2010**, *10*, 1329−1334.
(42) Janaky, C.; de Tacconi, N. R.; Chanmanee, W.; Rajeshwar, K. Electrodeposited Polyaniline in A Nanoporous WO_3 Matrix: An Organic/Inorganic Hybrid Exhibiting both p- And n-type Photoelectrochemical Activity. *J. Phys. Chem. C* **2012**, *116*, 4234−4242.
(43) Wei, H.; Zhu, J.; Wu, S.; Wei, S.; Guo, Z. Electrochromic Polyaniline/Graphite Oxide Nanocomposites with Endured Electrochemical Energy Storage. *Polymer* **2013**, *54*, 1820−1831.
(44) Baba, A.; Advincula, R. C.; Knoll, W. In Situ Investigations on the Electrochemical Polymerization and Properties of Polyaniline Thin Films by Surface Plasmon Optical Techniques. *J. Phys. Chem. B* **2002**, *106*, 1581−1587.
(45) Olenych, I. B.; Aksimentyeva, O. I.; Monastyrskii, L. S.; Pavlyk, M. R. Electrochromic Effect in Photoluminescent Porous Silicon Polyaniline Hybrid Structures. *J. Appl. Spectrosc.* **2012**, *79*, 495−498.
(46) Foot, P. J. S.; Simon, R. Electrochromic Properties of Conducting Polyanilines. *J. Phys. D: Appl. Phys.* **1989**, *22*, 1598−1603.
(47) Huang, W. S.; Humphrey, H. D.; MacDiarmid, A. G. Polyaniline, a Novel Conducting Polymer. *J. Chem. Soc., Faraday Trans. 1* **1986**, *82*, 2385−2400.
(48) Deepa, M.; Ahmad, S.; Sood, K. N.; Alam, J.; Ahmad, S.; Srivastava, A. K. Electrochromic Properties of Polyaniline Thin Film Nanostructures Derived from Solutions of Ionic Liquid/Polyethylene Glycol. *Electrochim. Acta* **2007**, *52*, 7453−7463.
(49) Rourke, F.; Crayston, J. A. Cyclic Voltammetry and Morphology of Polyaniline-Coated Electrodes Containing $[Fe(CN)_6]^{3-/4-}$ Ions. *J. Chem. Soc., Faraday Trans.* **1993**, *89* (2), 295−302.
(50) Bhadani, S. N.; Gupta, M. K.; Gupta, S. K. S. Cyclic Voltammetry and Conductivity Investigations of Polyaniline. *J. Appl. Polym. Sci.* **1993**, *49*, 397−403.
(51) Xiong, G.; Phua, S. L.; Dunn, B. S.; Ma, J.; Lu, X. Covalently Bonded Polyaniline TiO_2 Hybrids: A Facile Approach to Highly Stable Anodic Electrochromic Materials with Low Oxidation Potentials. *Chem. Mater.* **2010**, *22*, 255−260.
(52) Genies, E. M.; Lapkowski, M.; Penneau, J. F. Cyclic Voltammetry of Polyaniline: Interpretation of the Middle Peak. *J. Electroanal. Chem. Interfacial Electrochem.* **1988**, *249*, 97−107.
(53) Nunziante, P.; Pistoia, G. Factors Affecting the Growth of Thick Polyaniline Films by the Cyclic Voltammetry Technique. *Electrochim. Acta* **1989**, *34* (2), 223−228.
(54) Pruneanu, S.; Veress, E.; Marian, I.; Oniciu, L. Characterization of Polyaniline by Cyclic Voltammetry and UV-Vis Absorption Spectroscopy. *J. Mater. Sci.* **1999**, *34*, 2733−2739.
(55) Liu, X.; Zhou, A.; Dou, Y.; Pan, T.; Shao, M.; Han, J.; Wei, M. Ultrafast Switching of an Electrochromic Device Based on Layered Double Hydroxide/Prussian Blue Multilayered Films. *Nanoscale* **2015**, *7*, 17088.
(56) Runnerstrom, E. L.; Llordes, A.; Lounis, S. D.; Milliron, D. J. Nanostructured Electrochromic Smart Windows Traditional Materials and NIR-Selective Plasmonic Nanocrystals. *Chem. Commun.* **2014**, *50*, 10555.
(57) Yakuphanoglu, F.; Senkal, B. F. Electric and Thermoelectric Properties of Polyaniline Organic Semiconductor and Electrical Characterization of Al/PANI MIS Diode. *J. Phys. Chem. C* **2007**, *111*, 1840−1846.
(58) Chen, S. A.; Fang, Y.; Lee, H. T. Polyacrylic Acid-Doped Polyaniline as p-type Semiconductor in Schottky Barrier Electronic Device. *Synth. Met.* **1993**, *57*, 4082−4086.
(59) Bera, A.; Deb, K.; Kathirvel, V.; Bera, T.; Thapa, R.; Saha, B. Flexible Diode of Polyaniline/ITO Heterojunction on PET Substrate. *Appl. Surf. Sci.* **2017**, *418*, 264−269.
(60) Abdulrazzaq, O.; Bourdo, S. E.; Saini, V.; Watanabe, F.; Barnes, B.; Ghosh, A.; Biris, A. S. Tuning the Work Function of Polyaniline via Camphorsulfonic Acid: An X-ray Photoelectron Spectroscopy Investigation. *RSC Adv.* **2015**, *5*, 33.
(61) Sachtler, W. M. H.; Dorgelo, G. J. H.; Holscher, A. A. The Work Function of Gold. *Surf. Sci.* **1966**, *5*, 221−229.
(62) Zhang, Y.; Pluchery, O.; Caillard, L.; Lamic-Humblot, A. F.; Casale, S.; Chabal, Y. J.; Salmeron, M. Sensing the Charge State of Single Gold Nanoparticles via Work Function Measurements. *Nano Lett.* **2015**, *15*, 51−55.
(63) Pluchery, O.; Zhang, Y.; Benbalagh, R.; Caillard, L.; Gallet, J. J.; Bournel, F.; Lamic-Humblot, A. F. L.; Salmeron, M.; Chabal, Y. J.; Rochet, F. Static and Dynamic Electronic Characterization of Organic Monolayers Grafted on a Silicon Surface. *Phys. Chem. Chem. Phys.* **2016**, *18*, 3675.
(64) Misra, S. C. K.; Ram, M. K.; Pandey, S. S.; Malhotra, B. D.; Chandra, S. Vacuum-Deposited Metal/Polyaniline Schottky Device. *Appl. Phys. Lett.* **1992**, *61*, 1219.
(65) Durach, M.; Noginova, N. Spin angular momentum transfer and plasmogalvanic phenomena. *Phys. Rev. B: Condens. Matter Mater. Phys.* **2017**, *96*, 195411.
(66) Sheldon, M. T.; van de Groep, J. V.; Brown, A. M.; Polman, A.; Atwater, H. A. Plasmoelectric Potentials in Metal Nanostructures. *Science* **2014**, *346* (6211), 828−831.
(67) Liu, Y.; Goebl, J.; Yin, Y. Templated synthesis of nanostructured materials. *Chem. Soc. Rev.* **2013**, *42*, 2610−2653.
(68) Xiong, K.; Emilsson, G.; Maziz, A.; Yang, X.; Shao, L.; Jager, E. W. H.; Dahlin, A. B. Plasmonic metasurfaces with conjugated polymers for flexible electronic paper in Color. *Adv. Mater.* **2016**, *28*, 9956−9960.
(69) Atighilorestani, M.; Jiang, H.; Kaminska, B. Electrochromic-polymer-based switchable plasmonic color devices using surface-relief nanostructure pixels. *Adv. Opt. Mater.* **2018**, *6*, 1801179.

DOI: 10.1021/acsanm.9b00147
ACS Appl. Nano Mater. 2019, 2, 1713−1719